JBC RESEARCH ARTICLE

Contactin-1 is a critical neuronal cell surface receptor for perineuronal net structure

Received for publication, November 19, 2024, and in revised form, March 19, 2025 Published, Papers in Press, April 10, 2025,
https://doi.org/10.1016/j.jbc.2025.108504

Ashis Sinha[1], **Gabrielle Nickerson**[1], **Samuel Bouyain**[2,*,‡], **and Russell T. Matthews**[1,*,‡]

From the [1]*Department of Neuroscience and Physiology, State University of New York Upstate Medical University, Syracuse, New York, USA;* [2]*Division of Biological and Biomedical Systems, School of Science and Engineering, University of Missouri-Kansas City, Kansas City, Missouri, USA*

Reviewed by members of the JBC Editorial Board. Edited by Roger Colbran

Perineuronal nets (PNNs) are neuron-specific, mesh-like, substructures within the central nervous system extracellular matrix. They form on specific subsets of neurons and are well-established as key regulators of plasticity. The appearance of PNNs coincides with the developmental transition of the brain from a more to less plastic state with numerous studies implicating PNNs in regulating this transition. Additionally, recent work has also linked PNNs to several neuropsychiatric and neurodevelopmental disorders. However, despite this growing interest in PNNs, the mechanisms by which they modulate neural functions are poorly understood. This limited mechanistic understanding of PNNs is derived from the fact that there are limited models, tools, or techniques that specifically target PNNs without disrupting the surrounding neural extracellular matrix. Our work, therefore, focuses on understanding how PNNs form on the surface of cells with the ultimate goal of developing models and tools to manipulate and disrupt PNNs specifically. Here, using a phosphatidylinositol specific phospholipase-C, we first demonstrate that PNN components are bound to the cell surface by a glycosylphosphatidylinositol-linked receptor protein. Furthermore, we demonstrate, through the exogenous addition of WT and a mutant variant of phoshpacan to primary cortical neurons, that contactin-1 is the glycosylphosphatidylinositol-linked protein critical for retaining nets to the cell surface. We believe the identification of contactin-1 as a key cell-surface protein for PNN structure is a very significant step forward in our understanding of the formation and structure of nets. It will offer new strategies to dissect the assembly of this specialized neural matrix.

Perineuronal nets (PNNs) are a mesh-like conspicuous subcompartment of the neural extracellular matrix (ECM) occurring around the cell bodies and proximal dendrites of subsets of neurons in the central nervous system (CNS). PNNs are assembled as stable, mature synaptic circuitry is being established in the CNS, which closes the highly plastic critical period (CP) in the animal's neuronal development. A major driver behind the formation of nets is neuronal activity and, accordingly, decreased neuronal firing during early postnatal life leads to attenuated formation of PNNs. For example, rearing animals in complete darkness delays PNN formation and CP closure in the primary visual cortex and depriving sensory input by whisker trimming before CP closure leads to decreased PNN expression in the barrel cortex (1–4). Interestingly, if these procedures are carried out after CP closure no effects on PNNs are observed. The temporal appearance of PNNs during development and their activity-dependent formation has led investigators to postulate their involvement in the stabilization and maturation of synapses during development and in restricting plasticity in adult animals (1, 3, 5, 6). PNNs are particularly enriched in the glycosaminoglycan hyaluronan (HA) and HA-binding chondroitin sulfate proteoglycans. Digesting away PNNs by injecting bacterial chondroitinase ABC (ChABC), an enzyme capable of degrading the HA backbone of PNNs and the chondroitin sulfate chains of chondroitin sulfate proteoglycans, Pizzorusso *et al.* were able to reopen juvenile forms of plasticity in the visual cortex of adult rats (3). In addition to the cortex, a large amount of work has also demonstrated the role of PNNs in regulating plasticity across various other brain regions including the amygdala, hippocampus, striatum, and cerebellum (7–12). However, despite this increasing amount of evidence demonstrating the role of PNNs in regulating plasticity in the CNS, a mechanistic understanding of PNN function has been elusive.

The limited grasp of PNN function is derived primarily from our incomplete understanding of their structure and molecular composition and in turn, our inability to disrupt them specifically without also disrupting the surrounding ECM. Identifying the role of PNNs has relied primarily on enzymatic manipulation of these structures using ChABC. Though treatment with ChABC affects PNNs, it does not necessarily eliminate them and broadly disrupts any HA based ECM structure in the local area making it difficult to clearly delineate out the role of these enigmatic structures in the CNS. Additionally, almost all known PNN components are secreted molecules and are broadly expressed in the

‡ These authors contributed equally to this work.
* For correspondence: Russell T. Matthews, matthewr@upstate.edu; Samuel Bouyain, bouyains@umkc.edu.

neural ECM (13, 14). PNNs, however, are distinct from the surrounding ECM and form around only subsets of cells, specifically interneurons expressing the Ca^{2+}-binding protein parvalbumin. Genetic models targeting specific PNN components exist and have provided valuable insight into PNN function. However, to date they have focused on broadly secreted PNN components, and thus, a mechanism of PNN specificity has remained elusive (14–23). Therefore, the goal of our study is to provide a more complete understanding of PNN formation and structure. Critically, this includes identifying the cell surface receptors that are critical for PNNs.

We have previously demonstrated that receptor protein tyrosine phosphatase zeta (RPTPζ) is essential for PNN formation, as is its binding to the ECM glycoprotein tenascin-R (Tnr) (22, 24). Along with other existing data on PNN structure, our findings show that PNN components are immobilized on the neuronal surface by two distinct mechanisms. One is mediated by Tnr/RPTPζ complex while the other appears dependent on the HA backbone of PNNs. Both RPTPζ and Tnr are necessary for the lattice or net-like appearance of PNNs, and the absence of either leads to disrupted and aggregated PNN structures.

RPTPζ exists in multiple isoforms including transmembrane and secreted forms (25–27) but utilizing cultured neurons in which all forms of RPTPζ are eliminated (*Ptprz1* KOs), the disrupted PNN structure can be visualized by staining for the key PNN component aggrecan (21, 28, 29). In WT neuronal cultures aggrecan staining presents with a lattice-like pattern on the cell surface but is discontinuous and punctate in *Ptprz1* KO cultures (Fig. S1, (22)). But consistent with our previous studies, PNN structures on *Ptprz1* KO neurons are rescued by adding a soluble form of RPTPζ known as phosphacan (Fig. S1, (22)). And, importantly, PNN structures are similarly rescued using a recombinant form of RPTPζ that lacks the middle glycosaminoglycan attachment region (Fig. S1, (24)). These data confirm that a secreted form of RPTPζ, phosphacan, is critical for PNN structure. Furthermore these data demonstrate that the essential interactions mediated by phosphacan in PNNs are independent of its chondroitin sulfate chains and likely mediated by protein-protein interactions. However, they also suggests that for phosphacan, to mediate these effects in PNNs there must be additional proteins and potentially a cell surface receptor that links phosphacan to the neuronal surface in PNNs.

In this present study, we used biochemical approaches in primary cortical neurons to identify the receptor for this complex in PNNs as the glycosylphosphatidylinositol (GPI)-linked protein, contactin-1 (Cntn1). Consistent with these findings, KO of *Cntn1* is sufficient to dramatically alter PNN structure through disrupted binding of the Tnr/RPTPζ complex. To our knowledge, this is the first direct evidence uncovering the role of Cntn1 in PNN formation and the first identification of a cell surface receptor that is critical for PNN structure. The findings presented here provide novel insights into the structure and formation of PNNs and offer new strategies to manipulate them and better understand their function.

Results

Membrane binding of key PNN component aggrecan is partially dependent on a GPI-anchored protein

In our previous work, we developed a testable model of PNN structure. In this model, we hypothesized that a key PNN component, aggrecan, is bound to the HA backbone of PNNs by its N terminus and to Tnr by its C terminus in a Ca^{2+}-dependent manner (30–32). Tnr is then bound to phosphacan. Consistent with this model, our previously published work has demonstrated that protein-protein interactions between Tnr and phosphacan are essential for PNN structure. Phosphacan presumably would then be bound to the neuronal surface by a cell-surface protein. However, phosphacan is a known binding partner of several cell adhesion molecules such as Cntn1, Ng-CAM, N-CAM, and Nr-CAM (33–37). These cell surface receptors include both transmembrane proteins and GPI-anchored proteins. In order to narrow down the list of potential cell-surface binding partners for phosphacan in PNNs, we turned to a biochemical release assay we have developed in the lab (22). Using membranes isolated from adult mouse brain we determined that aggrecan, the most specific PNN component, is bound to the neuronal cell surface in PNNs by two distinct mechanisms, one dependent on the HA backbone, susceptible to enzymatic digestion of HA, and the other dependent on Ca^{2+} ions, susceptible to chelation by EDTA/EGTA (22). Importantly, we previously found that in membranes from *Ptprz1* KO brains, aggrecan binding became solely dependent on HA and was no longer also bound in a Ca^{2+}-dependent manner (22). We reasoned that if phosphacan was bound *via* a GPI-linked protein then cleaving the GPI-linkage with phosphatidylinositol-specific phospholipase-C (PIPLC) should be able to replace Ca^{2+} chelation in the release of aggrecan. If treatment with PIPLC did not lead to the release of aggrecan, then, we could rule out GPI-anchored proteins from being involved in binding phosphacan integrated into PNNs.

Membrane fractions from postnatal day 45 (PND 45) *Ptprz1* WT mouse brains were isolated and treated with ChABC to digest the HA backbone of PNNs, and/or EDTA to chelate Ca^{2+} ions, and/or PIPLC to disrupt any GPI links. After treatment, samples were centrifuged to obtain soluble release (R) and insoluble pellet (P) fractions and the release of aggrecan was analyzed by Western blot (Fig. 1*A*). We found significant differences in the release of aggrecan among the various treatment groups (one-way ANOVA $F(6, 16) = 61.31$, $p < 0.0001$) (Fig. 1*B*). As expected, aggrecan was partially released by ChABC treatment alone (54 ± 5%, $p < 0.0001$). However, a combination of ChABC and EDTA led to an almost complete release of aggrecan into the soluble phase (79 ± 7%, $p < 0.0001$). Interestingly, we also found that the majority of aggrecan is released into the soluble phase by ChABC and PIPLC treatment (86 ± 6%, $p < 0.0001$). Release of aggrecan by both ChABC and EDTA ($p < 0.0001$) and the ChABC and PIPLC treatment ($p < 0.0001$) was significantly higher than by ChABC treatment alone suggesting that in addition to the HA backbone of PNNs, aggrecan is bound to

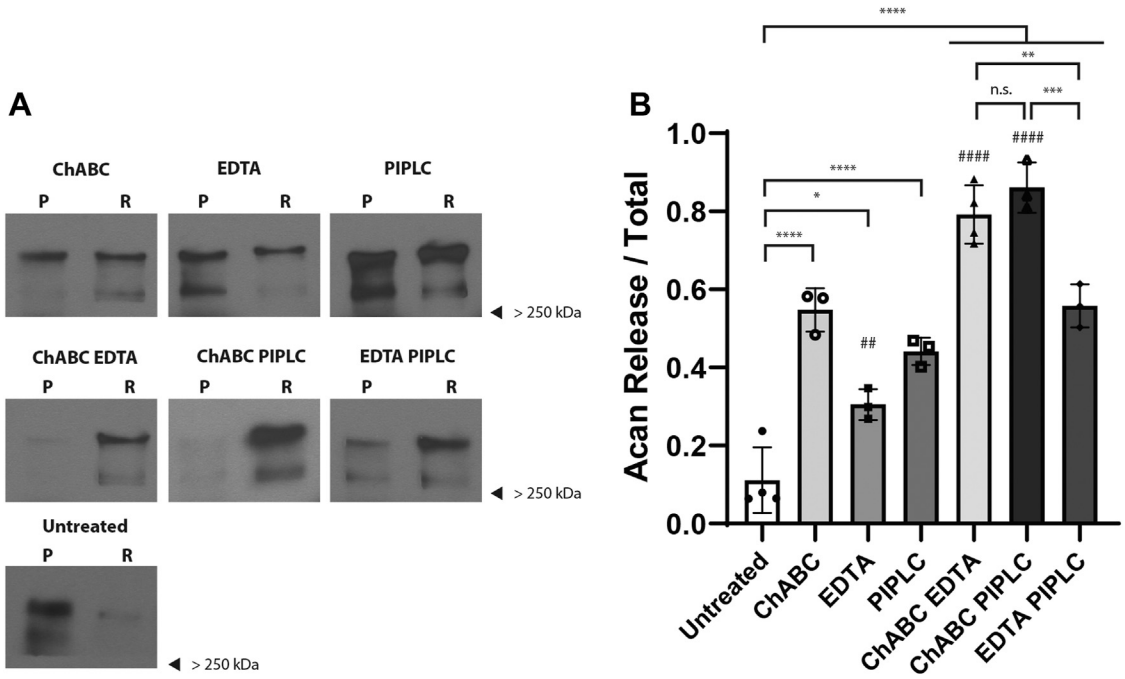

Figure 1. Membrane binding of key PNN component aggrecan depends on the HA backbone, Ca^{2+} ions, and a GPI-anchored protein. Homogenates PND 45 WT brains were treated with ChABC to digest the hyaluronan backbone of PNNs and/or EDTA to chelate Ca^{2+} ions and/or PIPLC to disrupt any GPI linked proteins. After treatment samples were centrifuged to obtain insoluble pellet (P) and soluble release (R) fractions. *A*, Western blotting image showing release of PNN marker aggrecan into soluble phase from brain homogenates of WT mice by ChABC, EDTA, and PIPLC treatment alone and combinations of ChABC EDTA, ChABC PIPLC, and EDTA PIPLC treatment. Aggrecan appears as a smear with two primary bands above 250 kDa that likely represent differential glycosylation and/or different cleavage products. *B*, there was a statistically significant difference in release of aggrecan across various treatment groups as determined by one-way ANOVA ($F(6, 16) = 61.31$, $p < 0.0001$). Aggrecan is partially released into the soluble fraction by ChABC (54 ± 5%, $p < 0.0001$), EDTA (30 ± 3%, $p = 0.0141$), and PIPLC (44 ± 3%, $p = 0.0001$) treatment alone as compared to untreated condition. However, aggrecan is almost completely released into the soluble phase by ChABC EDTA (79 ± 7%, $p < 0.0001$) and ChABC PIPLC treatment (86 ± 6%, $p < 0.0001$) as compared to the untreated group. Release of aggrecan by ChABC EDTA ($p < 0.0001$) and ChABC PIPLC treatment ($p < 0.0001$) was significantly greater than by ChABC treatment alone. Combination of EDTA PIPLC led to a significantly greater release of aggrecan than untreated group (55 ± 5%, $p < 0.0001$). However, it was not significantly different from treatment with ChABC, EDTA, or PIPLC alone. * in (*B*) indicates significance compared to untreated group unless denoted otherwise, # indicates comparison to ChABC treated group. Bar in graphs represent percentage release ± S.D. Individual data points are shown on the graphs. ChABC, chondroitinase ABC; GPI, glycosylphosphatidylinositol; HA, hyaluronan; PIPLC, phosphatidylinositol-specific phospholipase-C; PND, postnatal day; PNN, perineuronal net.

the cell membrane by Ca^{2+} dependent mechanism and a GPI anchor-dependent protein. EDTA (30 ± 3%, $p = 0.0141$) and PIPLC (44 ± 3%, $p < 0.0001$) treatment alone had significant effects on aggrecan release as well, indicating the role of these interactions in binding aggrecan to the cell surface.

We reasoned that if treatments with EDTA and PIPLC affected two distinct anchoring mechanisms, then the release of aggrecan with a combination of Ca^{2+} chelation and ablation of GPI anchors should be more significant than for each group alone. Combining these two treatments did result in a significant release of aggrecan as compared to the untreated group (55 ± 5%, $p < 0.0001$). However, the release was not significantly greater than the release in each of the individual treatments alone. Furthermore, treatments with EDTA, PIPLC, or a combination of the two were not significantly different from treatment with ChABC alone. These findings are consistent with the hypothesis that PNNs are immobilized to the cell membrane by two distinct mechanisms, one involving HA and the other involving Ca^{2+}. Results from these aggrecan-release experiments also indicate to us that a GPI-linked protein is critically involved in linking aggrecan to the cell membrane. We speculate that this GPI-anchored protein is part of the Ca^{2+}-dependent release mechanism of aggrecan and thus is implicated in the binding of phosphacan to the cell surface.

PNN components are immobilized on the cell surface, in part, by a GPI-linked protein

The Western blot analyses described above made us speculate that phosphacan is likely the PNN component that is bound *via* a GPI-linked protein and led us to form the model structure shown in Figure 2*A*. An interesting outcome of this model is that it predicts aggrecan would be released from PNNs by HA digestion combined with either Ca^{2+} chelation or PIPLC digestion but that the other components such as Tnr would likely only be released by combined treatments with PIPLC digestion and not with Ca^{2+} chelation. However, unlike aggrecan, Tnr is found both in PNNs and throughout the neural ECM so that we decided to test this hypothesis by analyzing the effects of ChABC, EDTA, and PIPLC treatments on PNN structure in cultured primary neurons.

Dissociated neuronal cultures present an attractive model to study interactions required for the formation of PNNs as they allow us to carry out our manipulations in live cells. Using this model system, we have previously shown that aggrecan staining in PNNs is profoundly disrupted by the combination of digestion of HA and chelation of Ca^{2+} but only slightly impacted with either treatment alone (22). Here, we additionally investigated if PIPLC could replace Ca^{2+} chelation in disrupting PNN structures. We found that treating cultured

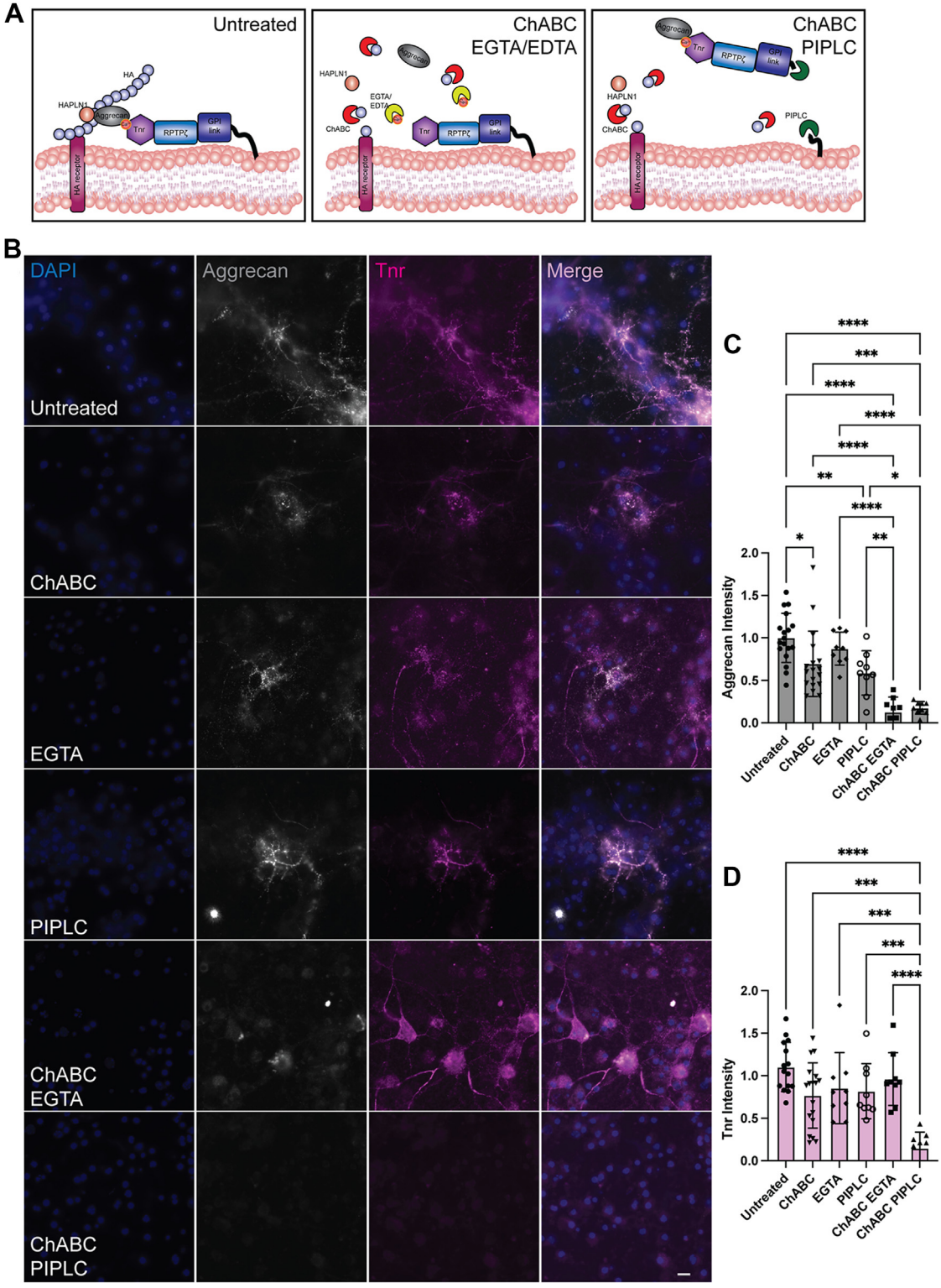

Figure 2. Treatment with ChABC and PIPLC eliminates staining for PNN components aggrecan and Tnr. *A*, based on our initial studies and work conducted previously, we created a model of PNN structure including a GPI-linked protein that tethers the structure to the cell surface. We hypothesize that aggrecan binds to Tnr, which is then bound to RPTPζ/phosphacan, and the entire complex is attached to the cell surface by a membrane receptor. The interaction of aggrecan and Tnr is known to be Ca^{2+} dependent, therefore, aggrecan is released by a combination of HA digestion and Ca^{2+} chelation, but Tnr bound to phosphacan and subsequently a membrane receptor (possibly a GPI-anchored protein) remains tethered to the cell membrane. We predict that combining HA digestion with PI lipid specific phospholipase-C (PIPLC) treatment will release both aggrecan and Tnr from the cell surface. *B*, to test this model, we turned to neuronal cell culture. Neurons derived from E16 WT mice were positive for PNN components aggrecan and Tnr. Acute treatment with ChABC, EGTA, or PIPLC alone only had small effects on aggrecan and Tnr levels. Treatment with ChABC to digest away the HA backbone of PNNs and EGTA to chelate Ca^{2+} ions in combination eliminated aggrecan staining but only had a minor effect on Tnr levels. Treatment with ChABC and PIPLC eliminated both aggrecan and Tnr staining. *C* and *D*, to quantify these findings, aggrecan and Tnr intensity for the different treatment groups relative to untreated condition was calculated and is presented here in a graphical form. Analysis by one-way ANOVA showed significant differences in levels of aggrecan and

neurons with either ChABC or EGTA only had small effects on aggrecan reactivity in PNNs (Fig. 2, *B* and *C*). Moreover, aggrecan levels under these treatment conditions were not significantly different from untreated controls. However, a combination of either ChABC and EGTA (loss = 87 ± 17%, $p < 0.0001$, Tukey's *post hoc* testing) or ChABC and PIPLC (loss = 82 ± 7%, $p > 0.0001$, Tukey's *post hoc* testing) led to an almost complete elimination of aggrecan staining.

Intriguingly, when we expanded these analyses to another essential PNN component, Tnr, the results provided greater insight into PNN structure (Fig. 2, *B* and *D*) and remained consistent with our model (Fig. 2*A*). The combination of ChABC and EGTA had no significant impact on Tnr levels (loss = 13 ± 14%, $p > 0.999$, Tukey's *post hoc* testing), whereas treating with ChABC and PIPLC essentially eliminated Tnr staining (loss = 85 ± 18%, $p < 0.0001$, Tukey's *post hoc* testing). As mentioned above, we hypothesized aggrecan is bound to the HA backbone of PNNs by its N terminus and to Tnr by its C terminus in a Ca^{2+} dependent manner. Tnr is then bound to phosphacan, and this complex is retained at the cell surface by a membrane receptor (Fig. 2*A*). Although aggrecan can be released by a combination of HA digestion and Ca^{2+} chelation, a complex of Tnr and phosphacan cannot be released because it remains tethered to the cell surface by a GPI-anchored protein. Combining HA digestion with PIPLC treatment releases both aggrecan and Tnr from the cell surface. Importantly, these results show that the protein tethering PNNs to the cell surface is a GPI-linked protein.

PNN structure can be disrupted by functionally blocking Cntn1

Our studies above indicated that a GPI-linked protein is critically involved in PNN structure and that treatment with PIPLC can replace Ca^{2+} chelation to disrupt PNN components. In our previous work, we showed that in *Ptprz1* KOs, PNNs are no longer bound to the neuronal surface in a Ca^{2+}-dependent manner and that Tnr and phosphacan form a key complex in PNNs (22, 24). Together these findings led us to believe that phosphacan binding in PNNs is dependent on a GPI-linked protein. To the best of our knowledge, the only GPI-linked protein that is known to interact with phosphacan is Cntn1 (36, 37). Interactions between RPTPζ/phosphacan and Cntn1 are essential to the maturation of oligodendrocyte precursor cells and are also known to promote the outgrowth of neurites in cultured neurons (35–37). Cntn1, however, has never previously been associated with PNNs.

As a first step to determine if Cntn1 might contribute to PNN structure, we utilized our primary neuronal culture model to determine if a function blocking antibody directed against Cntn1 could disrupt PNNs. As a control, we used an antibody directed against Cntn4. Importantly phosphacan interacts specifically with Cntn1 and does not bind with other members of the family, Cntn2-6 (36). As described above, we derived cultures from embryonic day 16 (E16) CD1 WT mice embryos and to block the interaction of any protein with Cntn1, we added an anti-Cntn1 polyclonal antibody (goat immunoglobulin G (IgG), final concentration of 2.5 μg/ml) or the same concentration of an anti-Cntn4 antibody to the cultures at 6 days *in vitro* (DIV 6) (38). We fixed the cells at DIV 9 and analyzed the binding of PNN component aggrecan with PNN peak/node analysis (22, 24). We identified aggrecan nodes or peaks using the local maxima function in ImageJ and determined the difference in intensity between the nodes and their surrounding space on the cell surface (mean node prominence) using an *ad hoc* algorithm. We found that untreated cells were positive for the PNN marker aggrecan and displayed regular PNN structures (Fig. 3). PNN staining in control cells (untreated and anti-Cntn4 antibody addition) appeared continuous with PNN peaks or nodes connected by bridge-like internode staining. In contrast, cells treated with the Cntn1 neutralizing antibody showed disrupted PNN structures (Fig. 3). PNN peaks in cultures where interaction with Cntn1 was blocked were significantly more prominent and isolated. Aggrecan staining appeared discontinuous and aggregated and resembled PNNs from *Ptprz1* KO cultures (Fig. S1) (one-way ANOVA $F(2, 46) = 7.63$., $p < 0.0014$, mean node prominence untreated = 5.55 ± 1.00, anti-Cntn1 antibody = 7.59 ± 2.45, $p = 0.0023$, anti-Cntn4 antibody = 5.71 ± 1.41, $p = 0.95$). Moreover, mean node prominence between anti-Cntn1 and anti-Cntn4 antibodies showed statistically significant differences ($p = 0.0078$). These results indicate that Cntn1 is required for proper binding of PNN components to the neuronal surface and is responsible for the regular lattice formation seen in untreated cells. Furthermore, these experiments demonstrate that binding of PNN components can be disrupted by blocking their interactions with Cntn1.

PNN structure depends on RPTPζ binding to Cntn1

As we have shown here (Fig. S1) and in previous studies (22), PNNs are disrupted in cultured neurons derived from *Ptprz1* KOs (22, 24). However, PNN structure can be restored by addition of brain-purified phosphacan or by addition of a recombinant truncated phosphacan construct. Importantly, previous structural work also provided atomic-level insights

Tnr among different treatment groups (aggrecan $F(5, 64) = 29.12$, $p < 0.0001$; Tnr $F(5, 63) = 9.92$, $p < 0.0001$). Tukey's *post hoc* testing showed significant loss of aggrecan but not Tnr with ChABC and EGTA treatment (aggrecan $p < 0.0001$; Tnr $p = 0.9123$). There was significant loss of both aggrecan and Tnr with ChABC and PIPLC treatment (aggrecan $p < 0.0001$; Tnr $p < 0.0001$). Tnr release was significantly greater with ChABC and PIPLC compared to ChABC and EGTA ($p < 0.0001$). These results indicate that aggrecan is immobilized on the cell surface by a HA-dependent mechanism then by a Ca^{2+} sensitive interaction and further downstream by a GPI anchor. Tnr on the other hand acts as an adapter molecule between aggrecan and the GPI anchor. Tnr is bound to the HA backbone through its interaction with aggrecan and remains attached to the cell surface by the GPI anchor when treated with ChABC and EGTA. Tnr staining is lost only when both the HA backbone and GPI anchor is disrupted by ChABC and PIPLC treatment. Bar in graphs represent percentage release ± S.D. Individual data points are shown on graphs. The scale bar represents 10 μm. * in (*C* and *D*) indicates significance. ChABC, chondroitinase ABC; E16, embryonic day 16; GPI, glycosylphosphatidylinositol; HA, hyaluronan; PIPLC, phosphatidylinositol-specific phospholipase-C; PNN, perineuronal net; RPTPζ, receptor protein tyrosine phosphatase zeta; Tnr, tenascin-R.

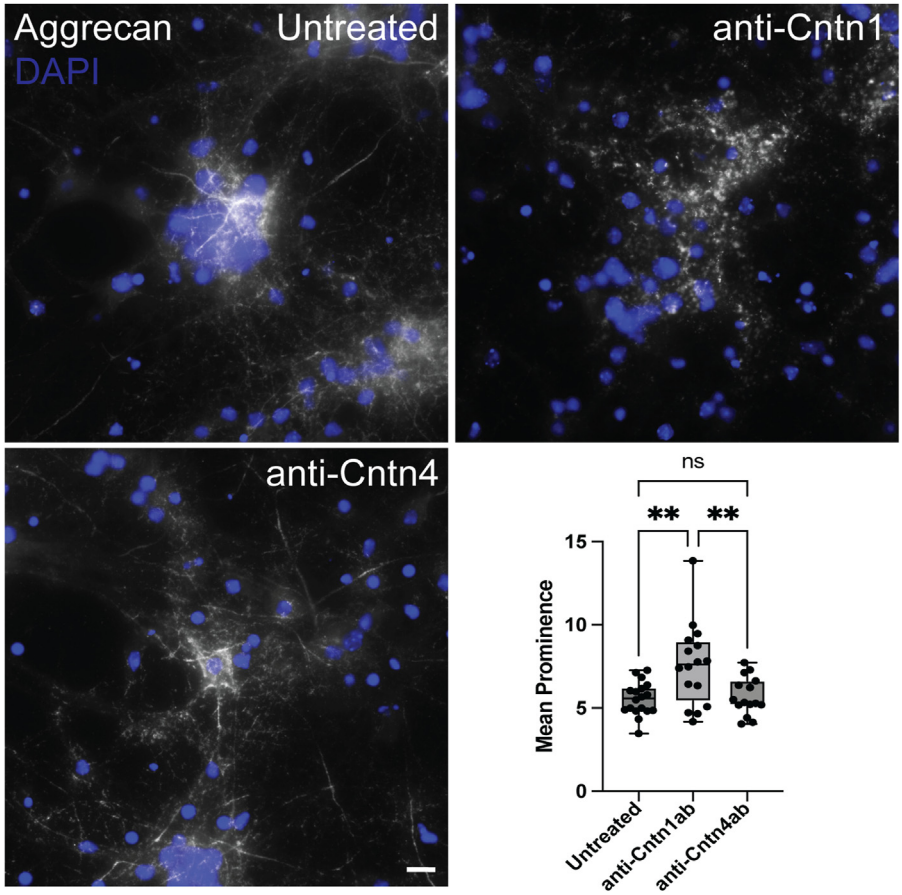

Figure 3. PNNs structure is disrupted when Cntn1 is functionally blocked in culture. Cortical cultures were derived from E16 WT mice. Cells were fixed at DIV 9, and PNNs were visualized by staining with PNN marker, aggrecan. PNNs staining appeared regular and continuous in untreated group. Addition of anti-Cntn1 function-blocking antibody (2.5 μg at DIV 6) resulted in disrupted and aggregated PNN structures and isolated PNN node/peaks. PNN structure was not disrupted by addition of anti-Cntn4 antibody (2.5 μg at DIV 6). Mean prominence or isolation of PNN peaks was quantified using our PNN node/peak analysis. Analysis by one-way ANOVA showed significant differences in the mean prominence index of PNNs (determined by the average isolation index of aggrecan staining peaks) among different treatment groups (aggrecan F (2, 46) = 7.63, p = 0.0014). Tukey's *post hoc* testing showed significant difference in mean prominence of aggrecan peaks between untreated and anti-Cntn1 antibody treatment group (p = 0.0023) and between anti-Cntn1 and anti-Cntn4 treatment (p = 0.0078). No significant difference was observed between untreated and anti-Cntn4 antibody treatment group (p = 0.9582). n = 15 to 20 PNNs per treatment group, 3 to 4 independent cultures. Individual data points are shown on graphs. The scale bar represents 10 μm. Cntn1, contactin-1; DIV, days *in vitro*; E16, embryonic day 16; PNN, perineuronal net

into the interaction between phosphacan and Cntn1 (36, 37). These studies demonstrated that a β-hairpin loop in the N-terminal carbonic anhydrase-like domain of phosphacan is critical for interacting with Cntn1. Using this information, the authors created a mutant form of phosphacan in which nine amino acids are deleted from this loop and that no longer interacts with Cntn1 (named here RPTPζ-βdel). Here, we compared the ability of the RPTPζ-βdel protein to recover PNN structure in cultured neurons compared to the wildtype RPTPζ protein (RPTPζ-WT). As described in neuronal cultures derived from E16, *Ptprz1* KO mice pups show irregular and aggregated staining for the PNN component aggrecan when fixed at 9 DIV (Fig. 4*A*). As expected, RPTPζ-WT protein added exogenously at 3 DIV recovered and restored aggrecan binding to the cell surface in *Ptprz1* KO neurons. In contrast, the Cntn1-binding mutant, RPTPζ-βdel, did not restore the PNN aggrecan structure in cultured neurons. To quantitatively assess this structural recovery, we utilized PNN peak/node analysis (Fig. 4*A*). We found statistically significant differences in mean PNN node prominence in our various treatment groups (one-way ANOVA F (2, 52) = 6.98, p = 0.0021). Addition of RPTPζ-WT recovered PNN structure in *Ptprz1* KO cells (mean node prominence: Untreated = 26 ± 7.29, RPTPζ-WT 19.55 ± 3.19, p = 0.0017, Tukey's *post hoc* testing). In contrast, RPTPζ-βdel did not restore the PNN aggrecan structure in *Ptprz1* KO cultured neurons, and aggrecan staining on cells continued to appear discontinuous and aggregated (mean node prominence = 23.91 ± 5.22, p = 0.4352). Moreover, mean node prominence between RPTPζ-WT and RPTPζ-βdel treatment groups also showed statistically significant differences (p = 0.0429). Together these data show that the binding of phosphacan to Cntn1 is critical for PNN structure.

Having determined that binding to Cntn1 is critical to recover PNN structure in *Ptprz1* KO neurons, we next asked if RPTPζ-βdel would act as a dominant negative and

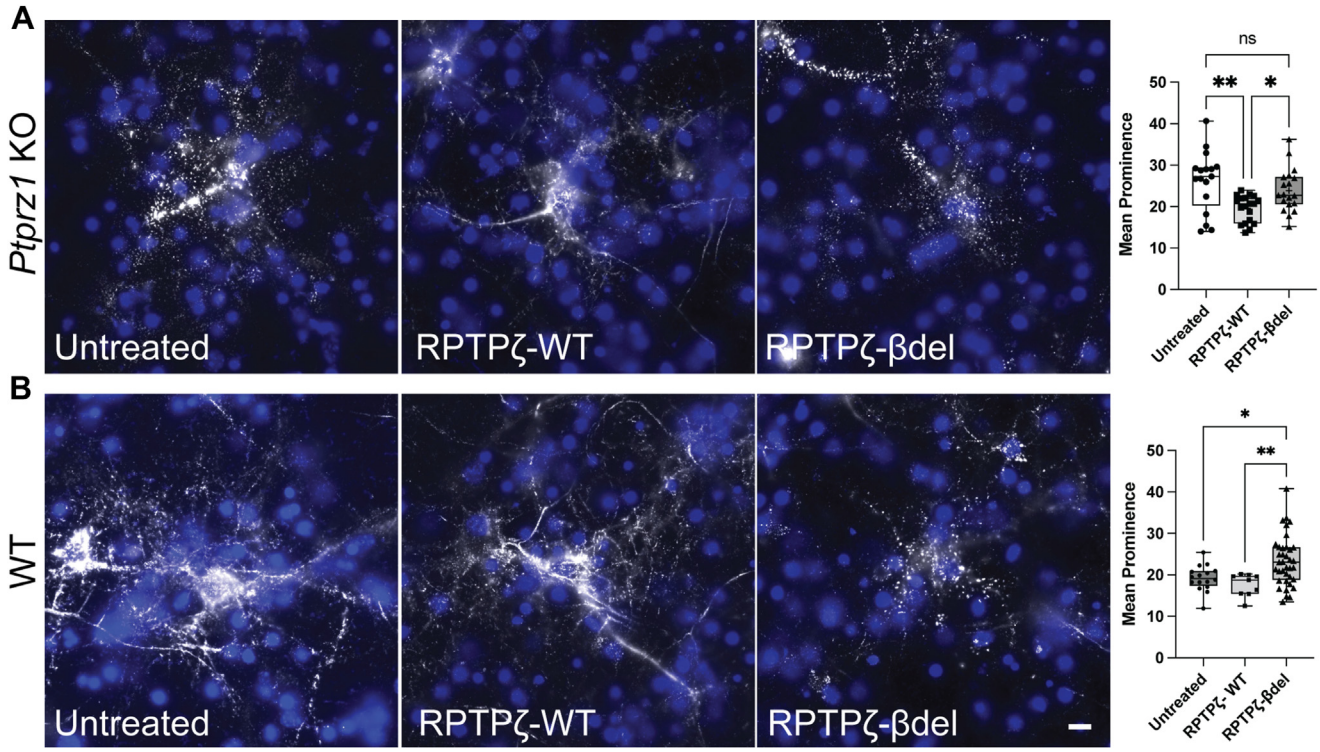

Figure 4. Addition of RPTPζ mutants is unable to recover PNN structure in RPTPζ-deficient *Ptprz1* KO neuronal cultures and disrupts PNNs in WT cultures. Cortical cultures from E16 *Ptprz1* KO mice lacking RPTPζ (*A*) or WT embryos (*B*) were derived and fixed at DIV 9. *A*, binding of PNN component aggrecan appeared disrupted with a broken and aggregated staining pattern in *Ptprz1* KO cultures. Addition of recombinant RPTPζ-WT (2 μg per well at DIV 3) to cells was able to restore aggrecan binding. Addition of Cntn1 binding mutant RPTPζ-βdel was unable to restore PNNs and aggrecan staining continued to appear broken and aggregated. Analysis by ordinary one-way ANOVA showed average isolation index of aggrecan staining nodes representing mean prominence of PNN staining peaks is significantly different among groups (F (2, 52) = 6.98, p = 0.0021). RPTPζ-WT-treated cells (n = 19 cells, three cultures) showed a significantly lower mean prominence (p = 0.0017) compared to untreated cells (n = 17 cells, three cultures) indicating more regular pattern of aggrecan staining and a decrease in node/peak isolation. Mean prominence of peaks in RPTPζ-βdel treated PNNs was not significantly different (n = 19 cells, four cultures, p = 0.4352) from untreated cells. Mean prominence of peaks in RPTPζ-βdel group was also significantly higher than RPTPζ-WT treated cells (p = 0.0429). *B*, cortical cultures derived from E16 WT mice fixed at DIV 9 and stained with PNN marker, aggrecan showed regular and continuous aggrecan staining in untreated group. Addition of RPTPζ-WT did not have any significant effects on aggrecan staining. Addition of RPTPζ-βdel (2 μg per well at DIV 6) resulted in disrupted and aggregated aggrecan staining. Analysis by ordinary one-way ANOVA showed significant differences in the mean prominence of PNNs (average isolation index of aggrecan staining peaks) among the various treatment groups (F (2, 59) = 6.91, p = 0.0020). Mean prominence is not significantly higher in RPTPζ-WT-treated cells (n = 9 PNNs, three cultures, p = 0.7201) as compared to untreated control cells (n = 15 cells, four cultures). On the other hand, mean prominence is significantly higher in RPTPζ-βdel treated cells (n = 37 PNNs, seven cultures, p = 0.0208) as compared to untreated control cells. Individual data points are shown on graphs. The scale bar represents 10 μm. Cntn1, contactin-1; DIV, days *in vitro*; E16, embryonic day 16; PNN, perineuronal net; RPTPζ, receptor protein tyrosine phosphatase zeta.

disrupt PNN structure in WT neurons (Fig. 4*B*). To quantitatively assess changes in PNN structure, we again utilized our PNN peak/node analysis (Fig. 4*B*). Here also, we found statistically significant differences in mean PNN node prominence among our various treatment groups (one-way ANOVA F (2, 59) = 6.915, p = 0.0020). In untreated WT neurons, aggrecan staining appeared normal (mean node prominence: untreated = 19.19 ± 3.10), and this was unaltered by the addition of RPTPζ-WT (mean node prominence: RPTPζ-WT = 17.56 ± 2.71, p = 0.8632). In contrast, addition of RPTPζ-βdel disrupted aggrecan staining and made it appear discontinuous and aggregated in appearance, similar to the aggrecan staining seen in *Ptprz1* KO neurons (mean node prominence: RPTPζ-βdel = 23.38 ± 6.03, p = 0.0003). Mean node prominence in RPTPζ-βdel treatment group was also significantly higher than RPTPζ-WT group (p = 0.0085). Together these data demonstrate that binding of phosphacan to Cntn1 is necessary for PNN structure.

PNN structure is disrupted in mice carrying null alleles for Cntn1

Our results from *in vitro* studies suggest that PNN components are immobilized to the neuronal surface by interacting with GPI-linked protein, Cntn1. If this is indeed true, then PNNs should appear disrupted in mice carrying null alleles for *Cntn1*. To verify this, we stained brain sections from *Cntn1*$^{-/-}$ (*Cntn1* KO) mice using the canonical PNN marker *Wisteria floribunda* agglutinin (WFA). Unfortunately, *Cntn1* KO mice die within 2 to 3 weeks after birth, making it difficult to study PNNs in these animals since this is a relatively early stage in PNN development (39). However, we were able to utilize animals at postnatal day 16 (PND16), which is a time point in which immature PNNs are beginning to form. WFA staining revealed immature PNN staining in the *Cntn1*$^{+/+}$ and *Cntn1*$^{+/-}$ (*Cntn1* WT and Het) brains were comparable. Strikingly, WFA staining appeared aggregated and punctate on the surface of neurons from *Cntn1* KO animals even at this early PNN developmental stage (Fig. 5*A*).

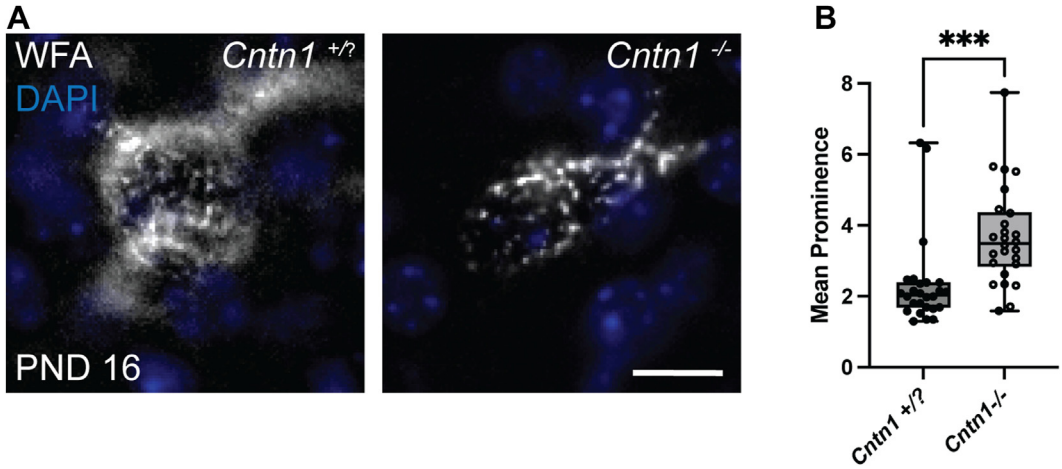

Figure 5. PNN structure is disrupted *in vivo* in mice carrying null alleles for *Cntn1*. *A*, in mice, PNNs first appear around the second postnatal week of life, presenting as diffuse structures around subsets of cells in the CNS. At PND 16, PNNs in *Cntn1* $^{+/+}$ and *Cntn1* $^{+/-}$ (combined here as *Cntn1*$^{+/?}$) animals cortices show typical developing WFA-positive PNN staining around subsets of interneuron. In contrast in *Cntn1* $^{-/-}$ cortices PNNs form but even at this early developmental time point appear disrupted. WFA staining in these brains is aggregated and punctate compared to the PNN staining seen in *Cntn1* $^{+/?}$ animals. *B*. Structural analyses using mean prominence or isolation of PNN peaks in these two groups were quantified using PNN node/peak analysis. There were significant differences in the mean prominence of PNNs between the two groups of animals. Mean prominence index was significantly higher in *Cntn1* $^{-/-}$ animals (*Cntn1* $^{-/-}$ = 3.68 ± 1.37, *Cntn1* $^{+/?}$ = 2.32 ± 1.22 and $p = 0.0005$, two-tailed Student's *t* test). Individual data points are shown on the graphs. Scale bar represents 10 μm. CNS, central nervous system; Cntn1, contactin-1; PND, postnatal day; PNN, perineuronal net; WFA, *Wisteria floribunda* agglutinin.

Our peak-node analysis revealed significant differences between *Cntn1* WT/Het and *Cntn1* KO animals. Mean prominence or isolation of PNN staining peaks was significantly higher in *Cntn1* KO animals (Fig. 5*B*, mean prominence *Cntn1* WT/Het = 2.32 ± 1.22 and *Cntn1* KO = 3.68 ± 1.37, $p < 0.0001$, two-tailed Student's *t* test).

Discussion

An incomplete understanding of PNN structure and consequently our inability to manipulate them specifically, and in a cell-autonomous manner, has been a major hurdle toward understanding their function in the CNS. The vast majority of PNN components that have been identified are secreted molecules, and most are broadly expressed in the CNS (2, 14, 16, 19, 20, 28, 40–48). Yet, PNNs are conspicuous structures that form around a small and discrete population of neurons that express the protein parvalbumin. The cell surface receptors responsible for PNN structure and their specific formation around unique subpopulations of neurons have remained unclear. In our previous studies, we identified two distinct interactions required for the proper formation of PNNs and demonstrated that PNN components bind to the neuronal surface by interacting with a HA backbone and through a complex formation involving Tnr and a soluble form of RPTPζ (22, 24). Here, we focused on determining how the RPTPζ/Tnr complex attaches to the neuronal cell surface in PNNs. We believe the identification of the key receptor for this complex, Cntn1, represents a major step forward in understand PNN structure and ultimately will provide a key insight into understanding PNN function. In this current study, we utilized biochemical analyses and cell biological studies to first demonstrate that the RPTPζ/Tnr complex is attached *via* a GPI-linked protein. In *Ptprz1* KO neuronal cultures, Tnr is lost from the cell surface which made us hypothesize Tnr is anchored to the surface by RPTPζ and therefore, we focused our work on identifying a cell surface receptor for RPTPζ (22). Previous work had identified interactions between RPTPζ and the GPI-linked protein Cntn1 (35) and provided a structural basis for them (36, 37). Subsequently using a combination of PIPLC, function blocking antibodies and a RPTPζ protein variant that does not bind Cntn1, we showed that the interaction of RPTPζ with Cntn1 is indeed required for PNN structure. Finally, we demonstrated that PNN structure is disrupted *in vivo* as well in Cntn1-deficient animals. Furthermore, the disrupted aspect of PNN structure in *Cntn1* KO mouse brains phenocopies the *Tnr* and *Ptprz1* KO PNN phenotypes. However, we should note that because *Cntn1* KOs only live to PND 16 to 18 we only could analyze the developmental role of Cntn1 in these KOs and subsequent studies will be critical to detail the role in plays in mature PNNs. Nonetheless, taken together, our work demonstrates that Cntn1 is critical in binding RPTPζ and RPTPζ/Tnr complexes in PNNs to the neuronal surface and that Cntn1 is critical for PNN structure. We believe this work is the first to identify a key cell surface receptor for PNNs.

This work combined with our previous studies enabled us to create an updated model of PNN structure that we believe represents an important step forward to understanding PNN structures and function (Fig. 6). Importantly key features of this model were validated in our current study. For example, we had previously shown that aggrecan is bound in PNNs in a HA- and Ca^{2+}- dependent manner (22). In contrast, here, we showed that despite the loss of aggrecan, Tnr remains bound to PNNs after HA digestion and Ca^{2+} chelation. Importantly, however, the combination of HA digestion and treatment with PIPLC eliminates both aggrecan and Tnr staining in PNNs. These results are predicted by our model and help highlight both the validity of the model and utility of using this model to direct future work on PNNs.

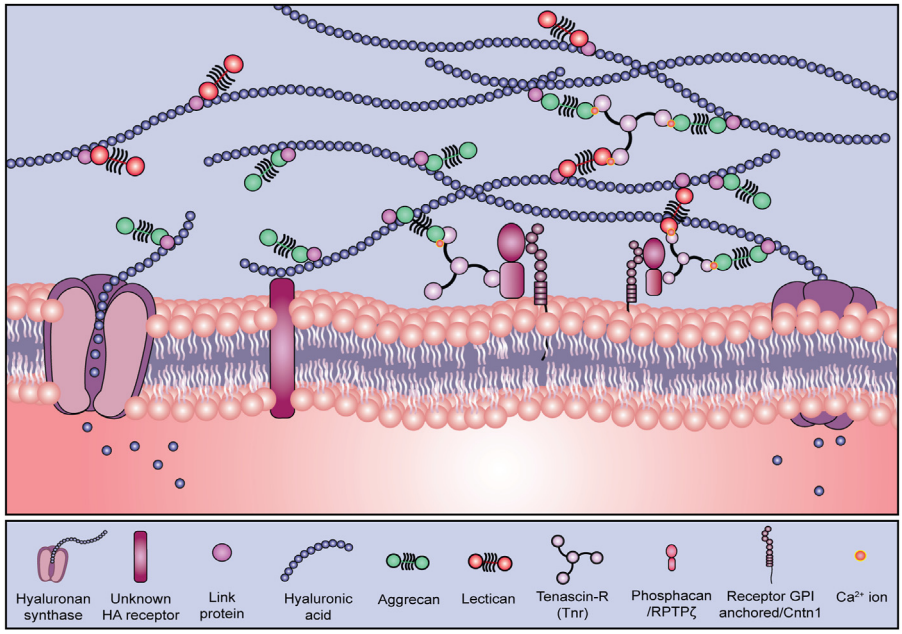

Figure 6. Proposed model of PNN structure. We propose a model for PNNs, in which lecticans are bound to the HA backbone and cross-linked to RPTPζ by Tnr. Our data suggest that it is the soluble form of RPTPζ, also known as phosphacan that mediates binding of PNN components to the cell surface. We present evidence that Cntn1 acts as a receptor for phosphacan in PNNs. To our knowledge this is the first direct demonstration of a PNN receptor. The mechanism by which HA binds to the cell surface is unknown and remains a goal of future studies. Cntn1, contactin-1; HA, hyaluronan; PNN, perineuronal net; RPTPζ, receptor protein tyrosine phosphatase zeta; Tnr, tenascin-R.

Our data demonstrate that Cntn1 plays an essential role in immobilizing PNNs to the cell surface. However, it was a surprise to us that Cntn1 plays this critical role in PNN structure given that it is broadly and highly expressed during neural development (39, 49). In other words, Cntn1 is by no means uniquely expressed in PNNs. Furthermore, Cntn1 plays a number of key roles in neural development (36, 37, 45, 50–52). It is well-known to play roles in axon growth and guidance, process fasciculation, oligodendrocyte development, and myelination and synapse formation. The critical role Cntn1 plays in other neural development processes is highlighted by the fact that *Cntn1* KO mice are severely runted in postnatal development and live to a maximum age of 16 to 18 days due to failure of peripheral nerve innervation (50). In contrast, PNNs form on a very selective and limited subset of interneurons (41). Although it is possible that a specific splice variant of Cntn1 may be expressed in PNN-bearing neurons, we do not believe Cntn1 is likely contributing to the cell-specificity of PNN formation *per se* but just to their structure. In support of this hypothesis, neurons that typically would have nets still stain positive for PNN components even in the *Ptprz1*, *Tnr*, and *Cntn1* knockouts, but PNN structure is disrupted from the typical reticular pattern to a more aggregated and punctate formation in these animals (15, 20, 22, 40, 46–48). Thus, we hypothesize that while a ternary complex of RPTPζ, Tnr, and Cntn1 is essential for PNN structure, it is likely that a HA-dependent binding of PNNs to the cell surface that gives these structures their cell-type specificity. This is an area we are currently actively investigating. In addition, because of the many functional roles of Cntn1, functional analysis of the impact of PNN disruption knockouts was not possible. This is a similar challenge with the *Ptprz1* KO and *Tnr* KO mice in which the expressed proteins function in PNNs but also in other systems making understanding their particular role in PNNs difficult or impossible with current models. We believe, however, that Cntn1 offers a key advantage going forward as it is a cell surface protein instead of a secreted protein. While secreted proteins can act at a distance from their cellular source, Cntn1 presumably acts in a cell autonomous manner. Therefore, conditional disruption of Cntn1 in PNN-bearing neurons could provide a unique tool to assess PNN functions. Overall, we believe this work provides an important step forward in understanding PNN structure and new insight into assessing PNN functions.

Experimental procedures

Animals

Mice lacking the *Ptprz1* gene (*Ptprz1* KO) were generated as previously described (53) and received from Dr Sheila Harroch (Department of Neuroscience, Institute Pasteur, Paris, France). For neuronal cultures, in addition to *Ptprz1* KO mice, timed pregnant CD-1 WT mice were purchased from Charles River Laboratories (Wilmington, MA, USA). All experiments carried out followed the protocols approved by the Institutional Animal Care and Use Committee of SUNY Upstate Medical University.

Antibodies

Mouse anti-tenascin-R 619 (MAB1624) and mouse anti-aggrecan (MAB11304) were purchased from R&D systems. Rabbit anti-aggrecan (AB1031) was purchased from Millipore

Sigma and was validated in aggrecan knockout animals. Function blocking goat anti-contactin1 (AF904) and sheep anti-contactin4 (AF5495) were purchased from R&D systems and validated against exogenously expressed proteins. Fluorescein labeled WFA was purchased from Vector Laboratories Inc.

Preparation of homogenates, soluble and insoluble fractions for biochemical release assay

Brain homogenates for release assay of PNN component aggrecan were derived from PND 45 *Ptprz1* WT brains. Tissue was homogenized in 150 mM sodium chloride and 50 mM Tris with EDTA-free protease inhibitor tablets (Roche, one tablet in 10 ml buffer), in a Potter-Elvehjem homogenizer. Homogenates were centrifuged at 8000*g* for 10 min at 4 °C. The supernatant was then removed, the pellet washed once and then resuspended in 1 ml buffer. A Bradford (Bio-rad) assay was performed, and protein concentrations were adjusted to 2.5 mg/ml. Samples were treated with 2 μl chondroitinase ABC (Sigma-Aldrich) and/or 5 μl PIPLC (Thermo Fisher Scientific) per 500 μl of sample and/or 1 mM EDTA for 8 h. Samples were centrifuged again at 8000*g* for 10 min at 4 °C to separate soluble release (R) fraction and insoluble pellet (P) fractions and subsequently prepared for Western blotting by adding sample loading buffer and heating to 95 °C for 5 min.

SDS-PAGE and Western blotting

Protein concentrations were determined by Bradford assay before gel electrophoresis. 6 to 15% gradient SDS-polyacrylamide gels were used and transferred to 0.45 μM nitrocellulose membranes. Western blotting was conducted as previously described (54). Briefly, blots were placed in blocking buffer composed of 5% milk in Tris-buffered saline with 0.1% Tween-20 and then incubated in primary antibody overnight. Blots were then incubated in horseradish peroxidase-conjugated secondary antibodies (The Jackson Laboratory) and exposed using supersignal west pico or femto chemiluminescent substrate (Thermo Fisher Scientific). Blots were imaged using Premium X-Ray film (Phenix Research Products).

Purification of phosphacan

Phosphacan was purified by anion exchange chromatography as previously described (22, 55). In brief, the soluble fraction, from PND 3 to 4 CD-1 mouse brain, was filtered using a polyvinylidene difluoride 0.22 μM filter, brought to a 0.5 M NaCl concentration, and run through a 1 ml HiTrap-Q HP column using a peristaltic pump connected to an Amersham Pharmacia RediFrac fraction collector (GE Healthcare Life Science). Sample was eluted over a continuous gradient of 0.5 M NaCl to 2.0 M NaCl over 10 column volumes and collected as 250 μl fractions. Fractions that were phosphacan rich, identified by dot blot analysis, were pooled, and concentrated using 100,000 MWCO Concentrators (Amicon Ultra, EMD Millipore). Approximately 250 ng of purified phosphacan was added to *Ptprz1 KO* cultures after the first medium change at 3 DIV, and 125 ng was added after the half-medium change at 6 DIV. Coverslips were fixed at 9 DIV and subsequently processed for immunocytochemistry.

Preparation of RPTPζ-WT-Fc and RPTPζ-βdel-Fc

Early passage HEK293 cells were plated on 10-cm dishes and transfected with RPTPζ-WT, RPTPζ-βdel constructs. Culture media were changed to Optimem, serum-free media 24 h post transfection. Media were collected 48 h post transfection and concentrated using 50,000 Da MWCO Concentrators (Amicon Ultra, EMD Millipore). Protein concentration was estimated using a Bradford assay (Bio-rad).

Primary cortical cultures

Neuronal primary cultures were prepared as previously described (19, 28). Briefly, cortices of E15 to 16 CD-1 WT or *Ptprz1* KO embryos were removed and digested in 0.25% trypsin-EDTA (Thermo Fisher Scientific). Mixed cells were filtered and suspended in Neurobasal medium with 3% B27, 1× Glutamax, and 1× penicillin-streptomycin (Thermo Fisher Scientific). Cells were then plated at a density of 2.1×10^6 cells/ml on coverslips (500 μl/per well) precoated with poly-D-lysine (50 μg/ml) and laminin (5 μg/ml) (Sigma-Aldrich) in a 24-well dish. To remove glia, cells were treated with 5 μM cytosine arabinoside (AraC, Sigma-Aldrich) at 1 DIV. The culture medium was then changed at 3 DIV to remove AraC and given a half change at 6 DIV. Cells were maintained at 37 °C/5% CO_2 until fixation. As per experimental requirements, coverslips were treated with 10 μl ChABC for 30 min and/or 2.5 mM EGTA for 15 min and/or PIPLC for 30 min for biochemical release assay of PNN components in neurons. Coverslips were fixed using 4% paraformaldehyde with 0.01% glutaraldehyde, pH 7.4 and subsequently processed for immunocytochemistry.

PNN recovery in RPTPζ-deficient cultures

Neuronal primary cultures were prepared as previously described from RPTPζ deficient, *Ptprz1* KO mice. Purified RPTPζ-WT or RPTPζ-βdel was added to cells at 2 μg/well of a 24 well dish at 3 DIV. Additional 1 μg/well was added after half media change at 6 DIV. Cells were fixed and analyzed at 9 DIV.

PNN disruption in CD1 WT cultures

Neuronal primary cultures were prepared as previously described from CD1 WT mice (19, 22, 24, 28). Purified RPTPζ-βdel (2 μg/well of a 24-well dish) or RPTPζ-WT (2 μg/well of a 24 well dish) or anti- Cntn1 antibody (AF904, affinity purified goat IgG) or anti-Cntn4 (AF5495, affinity purified sheep IgG) (2.5 μg/well of a 24-well dish) was added to cells at 6 DIV. Cells were fixed and analyzed at 9 DIV.

Immunocytochemistry

Primary cortical cultures plated on coverslips were fixed at 9 DIV in cold 4% phosphate-buffered paraformaldehyde with 0.01% glutaraldehyde, pH 7.4. Cells were then blocked in screening medium (Dulbecco's modified Eagle's medium, 5%

fetal bovine serum, and 0.2% sodium azide) for 1 h, before adding primary antibodies overnight at 4 °C. The following day, Alexa-fluor conjugated secondary antibodies (Thermo Fisher Scientific) in screening medium were added to the cells for 2 h before mounting the coverslips with ProLong antifade kit (Thermo Fisher Scientific). Cell nuclei were visualized with Hoechst solution (Thermo Fisher Scientific) diluted in 1× PBS. Coverslips were imaged using an epi-fluorescent Zeiss Imager.A2 with Nikon Elements software package. Final images were gathered and formatted using Fiji software (56) and assembled into figures using Adobe Photoshop and Adobe Illustrator.

Quantification and statistical analyses

PNN component intensity was calculated by taking large scan images (1200 μm × 900 μm) from three different areas for each coverslip. An (64 μm × 64 μm) area devoid of PNN staining was used for background subtraction and intensity was calculated using the measure function of ImageJ. PNN peak or node analysis was used to quantitatively describe the PNN aggregation seen on the surface of neurons in cultures derived from *Ptprz1* KO mice and CD-1 WT mice. PNN images (40 μm × 40 μm) were processed using the local maxima function of ImageJ to identify peaks ("nodes") of intense PNN staining. Once the nodes were identified, an *ad hoc* algorithm was used to measure the difference in intensity between the nodes, and their surrounding space on the cell surface (mean node prominence) was calculated and plotted for each genotype. Differences were found significant at $p < 0.05$ (unpaired Student's t test or analysis of variance (ANOVA) with Tukey's *post hoc* analyses as appropriate) using Graphpad Prism or RStudio statistical software. Analyses were conducted by an experimenter blinded to the experimental conditions.

Data availability

All experimental data that are not contained within the article or the supporting information are available by upon request by contacting the corresponding authors Russell T. Matthews (matthewr@upstate.edu) or Samuel Bouyain (bouyains@umkc.edu).

Supporting information—This article contains supporting information.

Author contributions—A. S., G. N., S. B., and R. T. M. visualization; A. S., G. N., S. B., and R. T. M. investigation; A. S., S. B., and R. T. M. methodology; A. S., S. B. and R. T. M. formal analysis; A. S., S. B., and R. T. M. writing–review and editing; A. S., S. B., and R. T. M. writing–original draft; A. S., S. B., and R. T. M. validation; S. B. and R. T. M. supervision; S. B. and R. T. M. software; S. B. and R. T. M. resources; S. B. and R. T. M. project administration; S. B. and R. T. M. funding acquisition; S. B. and R. T. M. data curation; S. B. and R. T. M. conceptualization

Funding and additional information—Research reported in this manuscript was supported by the National Institute of General Medical Sciences under award number R01 GM143757 (R. T. M. and S. B.). The content is solely the responsibility of the authors and does not necessarily represent the official views of the National Institutes of Health.

Conflicts of interest—The authors declare that they have no conflict of interest with the contents of this article.

Abbreviations—The abbreviations used are: ChABC, chondroitinase ABC; CNS, central nervous system; Cntn1, contactin-1; CP, critical period; DIV, days in vitro; E, embryonic day; ECM, extracellular matrix; GPI, glycosylphosphatidylinositol; HA, hyaluronan; gG, immunoglobulin; PIPLC, phosphatidylinositol-specific phospholipase-C; PND, postnatal day; PNN, perineuronal net; RPTPζ, protein tyrosine phosphatase receptor type Z; Tnr, tenascin-R.

References

1. Guimaraes, A., Zaremba, S., and Hockfield, S. (1990) Molecular and morphological changes in the Cat lateral geniculate nucleus and visual cortex induced by visual deprivation are revealed by monoclonal antibodies Cat-304 and Cat-301. *J. Neurosci.* **10**, 3014–3024
2. Lander, C., Kind, P., Maleski, M., and Hockfield, S. (1997) A family of activity-dependent neuronal cell-surface chondroitin sulfate proteoglycans in Cat visual cortex. *J. Neurosci.* **17**, 1928–1939
3. Pizzorusso, T., Medini, P., Berardi, N., Chierzi, S., Fawcett, J. W., and Maffei, L. (2002) Reactivation of ocular dominance plasticity in the adult visual cortex. *Science* **298**, 1248–1251
4. McRae, P. A., Rocco, M. M., Kelly, G., Brumberg, J. C., and Matthews, R. T. (2007) Sensory deprivation alters aggrecan and perineuronal net expression in the mouse barrel cortex. *J. Neurosci.* **27**, 5405–5413
5. Sur, M., Frost, D. O., and Hockfield, S. (1988) Expression of a surface-associated antigen on Y-cells in the Cat lateral geniculate nucleus is regulated by visual experience. *J. Neurosci.* **8**, 874–882
6. Pizzorusso, T., Medini, P., Landi, S., Baldini, S., Berardi, N., and Maffei, L. (2006) Structural and functional recovery from early monocular deprivation in adult rats. *Proc. Natl. Acad. Sci. U. S. A.* **103**, 8517–8522
7. Gogolla, N., Caroni, P., Lüthi, A., and Herry, C. (2009) Perineuronal nets protect fear memories from erasure. *Science* **325**, 1258–1261
8. Xue, Y. X., Xue, L. F., Liu, J. F., He, J., Deng, J. H., Sun, S. C., *et al.* (2014) Depletion of perineuronal nets in the amygdala to enhance the erasure of drug memories. *J. Neurosci.* **34**, 6647–6658
9. Végh, M. J., Heldring, C. M., Kamphuis, W., Hijazi, S., Timmerman, A. J., Li, K. W., *et al.* (2014) Reducing hippocampal extracellular matrix reverses early memory deficits in a mouse model of Alzheimer's disease. *Acta Neuropathol. Commun.* https://doi.org/10.1186/s40478-014-0076-z
10. Lee, H., Leamey, C. A., and Sawatari, A. (2012) Perineuronal nets play a role in regulating striatal function in the mouse. *PLoS One.* https://doi.org/10.1371/journal.pone.0032747
11. Slaker, M., Blacktop, J. M., and Sorg, B. A. (2016) Caught in the net: perineuronal nets and addiction. *Neural Plast.* https://doi.org/10.1155/2016/7538208
12. Carulli, D., Broersen, R., de Winter, F., Muir, E. M., Meškovic, M., de Waal, M., *et al.* (2020) Cerebellar plasticity and associative memories are controlled by perineuronal nets. *Proc. Natl. Acad. Sci. U. S. A.* **117**, 6855–6865
13. Carulli, D., Rhodes, K. E., Brown, D. J., Bonnert, T. P., Pollack, S. J., Oliver, K., *et al.* (2006) Composition of perineuronal nets in the adult rat cerebellum and the cellular origin of their components. *J. Comp. Neurol.* **494**, 559–577
14. Deepa, S. S., Carulli, D., Galtrey, C., Rhodes, K., Fukuda, J., Mikami, T., *et al.* (2006) Composition of perineuronal net extracellular matrix in rat brain: a different disaccharide composition for the net-associated proteoglycans. *J. Biol. Chem.* **281**, 17789–17800

15. Haunsø, A., Celio, M. R., Margolis, R. K., and Menoud, P.-A. (1999) Phosphacan immunoreactivity is associated with perineuronal nets around parvalbumin-expressing neurones. *Brain Res.* **834**, 219–222
16. Kwok, J. C. F., Carulli, D., and Fawcett, J. W. (2010) In vitro modeling of perineuronal nets: hyaluronan synthase and link protein are necessary for their formation and integrity. *J Neurochem* **114**, 1447–1459
17. Laabs, T., Carulli, D., Geller, H. M., and Fawcett, J. W. (2005) Chondroitin sulfate proteoglycans in neural development and regeneration. *Curr Opin Neurobiol* **15**, 116–120
18. Galtrey, C. M., Kwok, J. C. F., Carulli, D., Rhodes, K. E., and Fawcett, J. W. (2008) Distribution and synthesis of extracellular matrix proteoglycans, hyaluronan, link proteins and tenascin-R in the rat spinal cord. *Eur. J. Neurosci.* **27**, 1373–1390
19. Giamanco, K. A., and Matthews, R. T. (2012) Deconstructing the perineuronal net: cellular contributions and molecular composition of the neuronal extracellular matrix. *Neuroscience* **218**, 367–384
20. Morawski, M., Dityatev, A., Hartlage-Rübsamen, M., Blosa, M., Holzer, M., Flach, K., *et al.* (2014) Tenascin-R promotes assembly of the extracellular matrix of perineuronal nets *via* clustering of aggrecan. *Philosophical Trans. R. Soc. B: Biol. Sci.* https://doi.org/10.1098/rstb.2014.0046
21. Rowlands, D., Lensjø, K. K., Dinh, T., Yang, S., Andrews, M. R., Hafting, T., *et al.* (2018) Aggrecan directs extracellular matrix-mediated neuronal plasticity. *J. Neurosci.* **38**, 10102–10113
22. Eill, G. J., Sinha, A., Morawski, M., Viapiano, M. S., and Matthews, R. T. (2020) The protein tyrosine phosphatase RPTPξ/phosphacan is critical for perineuronal net structure. *J. Biol. Chem.* **295**, 955–968
23. Favuzzi, E., Marques-Smith, A., Deogracias, R., Winterflood, C. M., Sánchez-Aguilera, A., Mantoan, L., *et al.* (2017) Activity-dependent gating of parvalbumin interneuron function by the perineuronal net protein brevican. *Neuron* **95**, 639–655.e10
24. Sinha, A., Kawakami, J., Cole, K. S., Ladutska, A., Nguyen, M. Y., Zalmai, M. S., *et al.* (2023) Protein–protein interactions between tenascin-R and RPTPζ/phosphacan are critical to maintain the architecture of perineuronal nets. *J. Biol. Chem.* **299**, 104952
25. Garwood, J., Schnä, O., Clement, A., Schü Tte, K., Bach, A., and Faissner, A. (1999) DSD-1-Proteoglycan is the mouse homolog of phosphacan and displays opposing effects on neurite outgrowth dependent on neuronal lineage. *J. Neurosci.* **19**, 3888–3899
26. Garwood, J., Heck, N., Reichardt, F., and Faissner, A. (2003) Phosphacan short isoform, A novel non-proteoglycan variant of phosphacan/receptor protein tyrosine phosphatase-β, interacts with neuronal receptors and promotes neurite outgrowth. *J. Biol. Chem.* **278**, 24164–24173
27. Chow, J. P. H., Fujikawa, A., Shimizu, H., Suzuki, R., and Noda, M. (2008) Metalloproteinase- and γ-secretase-mediated cleavage of protein-tyrosine phosphatase receptor type Z. *J. Biol. Chem.* **283**, 30879–30889
28. Giamanco, K. A., Morawski, M., and Matthews, R. T. (2010) Perineuronal net formation and structure in aggrecan knockout mice. *Neuroscience* **170**, 1314–1327
29. [preprint] Grødem, S., Thompson, E. H., Røe, M. B., Vatne, G. H., Nymoen, I., Buccino, A., *et al.* (2024) Deciphering the role of aggrecan in parvalbumin interneurons: unexpected outcomes from a conditional ACAN knockout that eliminates WFA+ perineuronal nets. *bioRxiv*. https://doi.org/10.1101/2024.03.20.585910
30. Aspberg, A., Binkert, C., and Ruoslahtit, E. (1995) The versican C-type lectin domain recognizes the adhesion protein tenascin-R (J1-160/180/janusin). *Proc. Natl. Acad. Sci. U. S. A.* **92**, 10590–10594
31. Aspberg, A., Miura, R., Bourdoulous, S., Shimonaka, M., Heinegård, D., Schachner, M., *et al.* (1997) The C-type lectin domains of lecticans, a family of aggregating chondroitin sulfate proteoglycans, bind tenascin-R by protein-protein interactions independent of carbohydrate moiety. *Proc. Natl. Acad. Sci. U. S. A.* **94**, 10116–10121
32. Lundell, A., Olin, A. I., Mörgelin, M., Al-Karadaghi, S., Aspberg, A., and Logan, D. T. (2004) Structural basis for interactions between tenascins and lectican C-type lectin domains: evidence for a crosslinking role for tenascins. *Structure* **12**, 1495–1506
33. Milev, P., Fischer, D., Hä ring, M., Schulthess, T., Margolis, R. K., Chiquet-Ehrismann, R., *et al.* (1997) The fibrinogen-like globe of tenascin-C mediates its interactions with neurocan and phosphacan/protein-tyrosine phosphatase-zeta/beta. *J. Biol. Chem.* **272**, 15501–15509
34. Milev, P., Chiba, A., Häring, M., Rauvala, H., Schachner, M., Ranscht, B., *et al.* (1998) High affinity binding and overlapping localization of neurocan and phosphacan/protein-tyrosine phosphatase-zeta/beta with tenascin-R, amphoterin, and the heparin-binding growth-associated molecule. *J. Biol. Chem.* **273**, 6998–7005
35. Peles, E., Nativ, M., Lustig, M., Grumet, M., Schilling, J., Martinez, R., *et al.* (1997) Identification of a novel contactin-associated transmembrane receptor with multiple domains implicated in protein-protein interactions. *EMBO J.* **16**, 978–988
36. Bouyain, S., and Watkins, D. J. (2010) The protein tyrosine phosphatases PTPRZ and PTPRG bind to distinct members of the contactin family of neural recognition molecules. *Proc. Natl. Acad. Sci. U. S. A.* **107**, 2443–2448
37. Lamprianou, S., Chatzopoulou, E., Thomas, J. L., Bouyaing, S., and Harroch, S. (2011) A complex between contactin-1 and the protein tyrosine phosphatase PTPRZ controls the development of oligodendrocyte precursor cells. *Proc. Natl. Acad. Sci. U. S. A* **108**, 17498–17503
38. Mikami, T., Yasunaga, D., and Kitagawa, H. (2009) Contactin-1 is a functional receptor for neuroregulatory chondroitin sulfate-E. *J. Biol. Chem.* **284**, 4494–4499
39. Davisson, M. T., Bronson, R. T., Tadenev, A. L. D., Motley, W. W., Krishnaswamy, A., Seburn, K. L., *et al.* (2011) A spontaneous mutation in contactin 1 in the mouse. *PLoS One*. https://doi.org/10.1371/journal.pone.0029538
40. Haunsø, A., Ibrahim, M., Bartsch, U., Letiembre, M., Celio, M. R., and Menoud, P.-A. (2000) Morphology of perineuronal nets in tenascin-R and parvalbumin single and double knockout mice. *Brain Res.* **864**, 142–145
41. Matthews, R. T., Kelly, G. M., Zerillo, C. A., Gray, G., Tiemeyer, M., and Hockfield, S. (2002) Aggrecan glycoforms contribute to the molecular heterogeneity of perineuronal nets. *J. Neurosci.* **22**, 7536–7547
42. Oohashi, T., Hirakawa, S., Bekku, Y., Rauch, U., Zimmermann, D. R., Su, W. D., *et al.* (2002) Bral1, a brain-specific link protein, colocalizing with the versican V2 isoform at the nodes of Ranvier in developing and adult mouse central nervous systems. *Mol. Cell Neurosci.* **19**, 43–57
43. Bekku, Y., Su, W. D., Hirakawa, S., Fässler, R., Ohtsuka, A., Kang, J. S., *et al.* (2003) Molecular cloning of Bral2, a novel brain-specific link protein, and immunohistochemical colocalization with brevican in perineuronal nets. *Mol. Cell Neurosci.* **24**, 148–159
44. Deepa, S. S., Umehara, Y., Higashiyama, S., Itoh, N., and Sugahara, K. (2002) Specific molecular interactions of oversulfated chondroitin sulfate E with various heparin-binding growth factors: implications as a physiological binding partner in the brain and other tissues. *J. Biol. Chem.* **277**, 43707–43716
45. Çolakoğlu, G., Bergstrom-Tyrberg, U., Berglund, E. O., and Ranscht, B. (2014) Contactin-1 regulates myelination and nodal/paranodal domain organization in the central nervous system. *Proc. Natl. Acad. Sci. U. S. A.* https://doi.org/10.1073/pnas.1313769110
46. Gottschling, C., Wegrzyn, D., Denecke, B., and Faissner, A. (2019) Elimination of the four extracellular matrix molecules tenascin-C, tenascin-R, brevican and neurocan alters the ratio of excitatory and inhibitory synapses. *Sci. Rep.* https://doi.org/10.1038/s41598-019-50404-9
47. Mueller-Buehl, C., Reinhard, J., Roll, L., Bader, V., Winklhofer, K. F., and Faissner, A. (2022) Brevican, neurocan, tenascin-C, and tenascin-R act as important regulators of the interplay between perineuronal nets, synaptic integrity, inhibitory interneurons, and Otx2. *Front. Cell Dev. Biol.* https://doi.org/10.3389/fcell.2022.886527
48. [preprint] Dickens, S., Goodenough, A., and Kwok, J. (2022) An *in vitro* neuronal model replicating the *in vivo* maturation and heterogeneity of perineuronal nets. *bioRxiv*. https://doi.org/10.1101/2022.01.22.477344
49. Schweitzer, J., Gimnopoulos, D., Lieberoth, B. C., Pogoda, H. M., Feldner, J., Ebert, A., *et al.* (2007) Contactin1a expression is associated with oligodendrocyte differentiation and axonal regeneration in the central nervous system of zebrafish. *Mol. Cell Neurosci.* **35**, 194–207
50. Berglund, E. O., Murai, K. K., Fredette, B., Sekerková, G., Marturano, B., Weber, L., *et al.* (1999) Ataxia and abnormal cerebellar microorganization in mice with ablated contactin gene expression. *Neuron* **24**, 739–750

51. Boyle, M. E., Berglund, E. O., Murai, K. K., Weber, L., Peles, E., and Ranscht, B. (2001) Contactin orchestrates assembly of the septate-like junctions at the paranode in myelinated peripheral nerve. *Neuron* **30**, 385–397
52. Chen, Y. A., Lu, I. L., and Tsai, J. W. (2018) Contactin-1/F3 regulates neuronal migration and morphogenesis through modulating rhoa activity. *Front Mol Neurosci*. https://doi.org/10.3389/fnmol.2018.00422
53. Harroch, S., Palmeri, M., Rosenbluth, J., Custer, A., Okigaki, M., Shrager, P., *et al.* (2000) No obvious abnormality in mice deficient in receptor protein tyrosine phosphatase β. *Mol Cell Biol.* **20**, 7706–7715
54. Viapiano, M. S., Matthews, R. T., and Hockfield, S. (2003) A novel membrane-associated glycovariant of BEHAB/brevican is up-regulated during rat brain development and in a rat model of invasive glioma. *J. Biol. Chem.* **278**, 33239–33247
55. Dwyer, C. A., Baker, E., Hu, H., and Matthews, R. T. (2012) RPTPζ/phosphacan is abnormally glycosylated in a model of muscle-eye-brain disease lacking functional POMGnT1. *Neuroscience* **220**, 47–61
56. Schindelin, J., Arganda-Carreras, I., Frise, E., Kaynig, V., Longair, M., Pietzsch, T., *et al.* (2012) Fiji: an open-source platform for biological-image analysis. *Nat. Methods* **9**, 676–682